An analytical solution for modeling thermal energy transfer in a confined aquifer system

Yang Shaw-Yang · Yeh Hund-Der

Abstract A mathematical model is developed for simulating the thermal energy transfer in a confined aquifer with different geological properties in the underlying and overlying rocks. The solutions for temperature distributions in the aquifer, underlying rock, and overlying rock are derived by the Laplace transforms and their corresponding time-domain solutions are evaluated by the modified Crump method. Field data adopted from the literature are used as examples to demonstrate the applicability of the solutions in modeling the heat transfer in an aquifer thermal energy storage (ATES) system. The results show that the aquifer temperature increases with time, injection flow rate, and water temperature. However, the temperature decreases with increasing radial and vertical distances. The heat transfer in the rocks is slow and has an effect on the aquifer temperature only after a long period of injection time. The influence distance depends on the aquifer physical and thermal properties, injection flow rate, and injected water temperature. A larger value of thermal diffusivity or injection flow rate will result in a longer influence distance. The present solution can be used as a tool for designing the heat injection facilities for an ATES system.

Keywords Thermal energy storage · Groundwater flow · Analytical solution · Laplace transform · Heat transfer

Received: 18 October 2007 / Accepted: 27 May 2008
Published online: 16 July 2008

Y. Shaw-Yang
Department of Civil Engineering,
Vanung University,
No. 1 Van Nung Rd., Chungli 320, Taiwan, Republic of China

Y. Hund-Der (✉)
Institute of Environmental Engineering,
National Chiao Tung University,
1001 University Rd., Hsinchu 300, Taiwan, Republic of China
e-mail: hdyeh@mail.nctu.edu.tw
Fax: +886-3-5726050

Introduction

The global climate change is a worldwide and growing concern at the present time. Green energies have been considered as alternatives for reducing the discharge of the carbon dioxide (CO_2) and heat emission into the atmosphere. Geothermal energy is one of the natural resources and has been utilized in several forms for a long time, e.g., hot spring, thermal spring, warm spring, hot vapor, etc. The use of geothermal energy is currently limited to a small number of the conventional geothermal steam and hot water reservoirs. The aquifer thermal energy storage (ATES) is one of the techniques dealing with the waste heat. This technique involves storing the excess waste heat in an aquifer and recovering it as needed. In other words, the ATES system can store the waste heat produced from industrial activities as a hot water source for future use.

For the problem of heat exchanger, Carslaw and Jaeger (1959) considered a case of a moving hot fluid over a semi-infinite solid with the surface temperature of the solid equaling to the temperature of the fluid at any point. They gave the solutions of the temperature in the fluid and solid in the Cartesian coordinate system. Cheng and Teckchandani (1977) studied the transient heating and fluid withdrawal in a liquid-dominated geothermal reservoir of an island aquifer. They demonstrated the contraction of the isotherms in a reservoir due to fluid withdrawal from both a line and a plan sink. Bodvarsson et al. (1982) developed a two-dimensional model of the vertical fault-charged hydrothermal systems including the effects of heat losses to the confining layers. Their model was used in theoretical studies and applied to estimate the temperature distribution at Susanville, California. Ziagos and Blackwell (1986) developed a mathematical model for the transient temperature effects of horizontal fluid flow in geothermal systems. An approximate analytical solution was derived using the Laplace transforms and compared to a Fourier transform solution. Their solution reduces to the solution of Bodvarsson et al. (1982) when the lower rock has a finite thickness and a fixed temperature specified as a boundary condition.

Bodvarsson and Tsang (1982) considered the problem of cold-water injection into a geothermal reservoir with a number of equally spaced horizontal fractures. The Laplace-domain solutions for the fracture and rock temperatures are derived by the Laplace transforms and

 DOI 10.1007/s10040-008-0327-9

calculated via a numerical inverter of Stehfest (1970). Chen and Reddell (1983) developed analytical solutions describing steady and transient temperature distributions for thermal injection into a radial confined aquifer. The thermal injection system was assumed symmetrical with respect to the mid-plane of the aquifer with the same thickness of the caprock and bedrock. A graphical technique was provided for evaluating the thermal properties of the aquifer. Palmer et al. (1992) conducted a thermal energy injection and storage experiment in an unconfined aquifer to provide the field data of numerical simulation at the Canadian Force Base Borden site. Molson et al. (1992) presented a three-dimensional finite element model for describing the coupled density-dependent groundwater flow and the thermal energy transport. Their model can simulate the low-temperature thermal energy transport system that arises in connection with the ATES and heat-extraction systems. Chevalier and Banton (1999a) developed a random walk model for heat transfer for a single injection well in a confined aquifer system. Their results were compared with the analytical solution given by Avdonine and Rubinstein in Noyer (1977) and finite difference model. Chevalier and Banton (1999b) also applied the random walk method to thermal energy storage in fractured aquifers. Nagano et al. (2002) investigated the influence of natural convection on forced horizontal flow in saturated media for an ATES system using both the experiments and computer simulations. They stated that both natural convection and temperature dependence of water viscosity are required in the simulation of an ATES. Paksoy et al. (2004) compared the performance of heat, ventilation and air-conditioning (HVAC) system integrated with ATES for a supermarket in Turkey with a conventional system. The result shows that the HVAC system with ATES has almost 60% higher operating efficiency than a conventional one. Stopa and Wojnarowski (2006) developed an analytical model of cold water front movement in a geothermal reservoir by assuming that the rock density and heat capacity are functions of temperature. The method of characteristics was used to find the discontinuous solutions. In addition, they also presented a velocity equation of thermal front in a cold-water injection system; however, the equation did not apply to the case of hot water injection into a colder reservoir.

The objective of this study is to propose a mathematical model for describing the heat transfer in a confined aquifer which has different geological properties in the underlying and overlying rocks. The Laplace-domain solutions of the temperature distribution are derived by the Laplace transforms and their corresponding time-domain solutions are obtained using the modified Crump method (de Hoog et al. 1982). The solutions can be used to predict the temperature distribution in an ATES system.

Mathematical model

An idealized representation of an injection well in a confined aquifer is shown in Fig. 1. The hot water is injected into the confined aquifer through the well and flows between the underlying and overlying rocks. Heat is transferred from water to the rocks and is stored in the confined aquifer. The assumptions made in the mathematical model are:

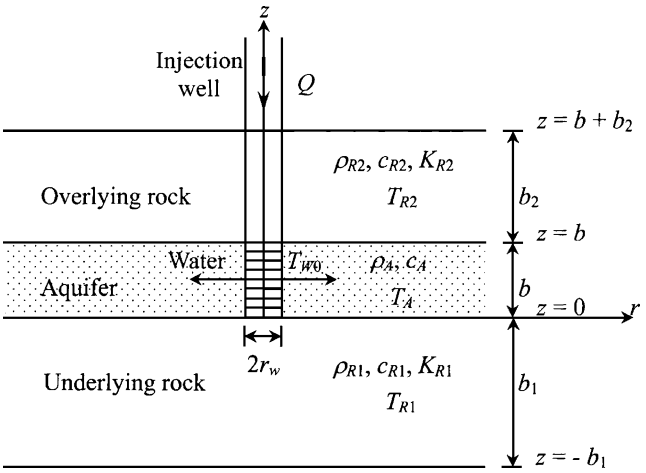

Fig. 1 Schematic diagram of the thermal energy storage in a porous aquifer

1. The aquifer is homogeneous, isotropic, infinite in horizontal extent, and of a constant thickness. In addition, the temperature in the aquifer is considered well-mixed over the entire thickness.
2. The overlying and underlying rocks are homogeneous, isotropic, impermeable, and of constant thicknesses.
3. The mass flow is assumed to be steady and the hot water is injected at a constant rate into the aquifer through a fully penetrating well.
4. The physical density, specific heat, and thermal conductivity of the aquifer, overlying rock, and underlying rock are assumed constants. This assumption is applicable when the change of temperatures in the rocks and water flow is not very large (Stopa and Wojnarowski 2006).
5. The heat transfer by horizontal convection occurs along the radial direction and by vertical thermal conduction in the overlying and underlying rocks.
6. The temperatures of the aquifer, underlying rock, and overlying rock are initially constant. Assuming that the injection well is insulated, i.e., the heat loss of the injection water to the overlying rock is negligible; therefore, the temperature of injection water is maintained constant.
7. The lower boundary of underlying rock and the upper boundary of overlying rock are fractures and the fluid temperatures in the fractures are maintained constant.

Under a typical laminar flow condition, the heat transfer is dominated by advection in the aquifer and by diffusion in the confining rocks (Cheng et al. 2001). Thus, the effects of heat dispersion in the aquifer are neglected in this study. For the aquifer, the governing equation describing the steady-state temperature distribution in a

 DOI 10.1007/s10040-008-0327-9

radial confined aquifer system can be formulated by applying the energy balance law as (Özisik 1993)

$$\left(\pi r^2 b\right)\rho_A c_A\left[v\frac{\partial T_A(r,t)}{\partial r}\right] = \left(\pi r^2\right)\left[-K_{R1}\left.\frac{\partial T_{R1}(r,z,t)}{\partial z}\right|_{z=0} + K_{R2}\left.\frac{\partial T_{R2}(r,z,t)}{\partial z}\right|_{z=b}\right] \tag{1}$$

where $T_A(r, t)$ is the temperature of aquifer; $T_{R1}(r, z, t)$ and $T_{R2}(r, z, t)$ are the temperatures of the underlying and overlying rocks, respectively; K_{R1} and K_{R2} are the thermal conductivities of the underlying and overlying rocks, respectively; b is the thickness of the confined aquifer; ρ_A is the density of fluid-saturated aquifer; c_A is the specific heat of the fluid-saturated aquifer; r is the radial distance from the injection well; z is the vertical distance along the injection well; and t is the time. The flow velocity, v, is $Q/(2\pi rb)$ where Q is the constant volumetric injection rate.

The initial temperature of the aquifer T_{A0} is assumed constant, that is

$$T_A(r,0) = T_{A0} \tag{2}$$

The boundary condition for the temperature at the well screen is

$$T_A(r_w,t) = T_{W0} \tag{3}$$

where T_{W0} is the temperature of the injected water.

The conduction equation for the temperature distribution in the underlying rock can be written as

$$\frac{\partial^2 T_{R1}(r,z,t)}{\partial z^2} = \frac{\rho_{R1}c_{R1}}{K_{R1}}\frac{\partial T_{R1}(r,z,t)}{\partial t} \tag{4}$$

where ρ_{R1} and c_{R1} are the density and specific heat of the underlying rock, respectively.

Neglecting the geothermal gradient, the initial temperature of the underlying rock T_{R10} can be expressed as

$$T_{R1}(r,z,0) = T_{R10} \tag{5}$$

The boundary conditions for the underlying rock are

$$T_{R1}(r,0,t) = T_A(r,t), \text{for the upper boundary} \tag{6}$$

and

$$T_{R1}(r,-b_1,t) = T_{R10}, \text{for the lower boundary} \tag{7}$$

Similarly, the conduction equation for the temperature distribution in the overlying rock can be written as

$$\frac{\partial^2 T_{R2}(r,z,t)}{\partial z^2} = \frac{\rho_{R_2}c_{R2}}{K_{R2}}\frac{\partial T_{R2}(r,z,t)}{\partial t} \tag{8}$$

where ρ_{R2} and c_{R2} are the density and specific heat of the overlying rock, respectively.

The initial temperature of the overlying rock T_{R20} when neglecting the geothermal gradient is

$$T_{R2}(r,z,0) = T_{R20} \tag{9}$$

The boundary conditions for the overlying rock are

$$T_{R2}(r,b,t) = T_A(r,t), \text{for the lower boundary} \tag{10}$$

and

$$T_{R2}(r,b+b_2,t) = T_{R20}, \text{for the upper boundary} \tag{11}$$

The detailed derivations for the Laplace transform solutions to Eqs. (1)–(11) are given at the end (see Appendix). The dimensionless parameters used hereinafter are defined as

$$\begin{aligned} T_{AD}(r,t) &= \tfrac{T_A(r,t)-T_{A0}}{T_{W0}-T_{A0}}, \alpha_{R1} = \tfrac{K_{R1}}{\rho_{R1}c_{R1}}, \alpha_{R2} = \tfrac{K_{R2}}{\rho_{R2}c_{R2}}, \\ T_{R1D}(r,z,t) &= \tfrac{T_{R1}(r,z,t)-T_{A0}}{T_{W0}-T_{A0}}, T'_{R1D}(r,z,t) = T_{R1D}(r,z,t) - T_{R10D}, \\ T_{R10D} &= \tfrac{T_{R10}-T_{A0}}{T_{W0}-T_{A0}} \\ T_{R2D}(r,z,t) &= \tfrac{T_{R2}(r,z,t)-T_{A0}}{T_{W0}-T_{A0}}, T'_{R2D}(r,z,t) = T_{R2D}(r,z,t) - T_{R20D}, \\ T_{R20D} &= \tfrac{T_{R20}-T_{A0}}{T_{W0}-T_{A0}} \end{aligned} \tag{12}$$

Based on Eq. (12), Eqs. (1)–(11) can be expressed in dimensionless forms. The solution for the dimensionless temperature of the aquifer is

$$\overline{T}_{AD}(r,s) = \left(\frac{1}{s} - \frac{A_2(s)}{sA_1(s)}\right)\exp\left\{\left(\frac{-\pi}{\rho_A c_A Q}\right)A_1(s)\left(r^2 - r_w^2\right)\right\} + \frac{A_2(s)}{sA_1(s)} \tag{13}$$

with

$$A_1(s) = K_{R1}q_1\coth(q_1b_1) + K_{R2}q_2\coth(q_2b_2) \tag{14}$$

and

$$A_2(s) = K_{R1}q_1\coth(q_1b_1)T_{R10D} + K_{R2}q_2\coth(q_2b_2)T_{R20D} \tag{15}$$

where s is the Laplace variable (Spiegel 1965), $q_1^2 = s/\alpha_{R1}$, and $q_2^2 = s/\alpha_{R2}$. In addition, the Laplace-domain solutions for the dimensionless temperature are

$$\overline{T}_{R1D}(r,z,s) = \frac{\sinh(q_1(b_1+z))}{\sinh(q_1b_1)}\left(\overline{T}_{AD}(r,s) - \frac{T_{R10D}}{s}\right) + \frac{T_{R10D}}{s} \tag{16}$$

for the underlying rock and

$$\overline{T}_{R2D}(r,z,s) = \frac{\sinh(q_2(b+b_2-z))}{\sinh(q_2b_2)}\left(\overline{T}_{AD}(r,s) - \frac{T_{R20D}}{s}\right) + \frac{T_{R20D}}{s} \tag{17}$$

for the overlying rock.

DOI 10.1007/s10040-008-0327-9

In order to express Eqs. (13)–(17) in dimensionless forms, following dimensionless variables are introduced:

$$r_D = \frac{r}{b}, r_{wD} = \frac{r_w}{b}, z_D = \frac{z}{b}, b_{1D} = \frac{b_1}{b}, b_{2D} = \frac{b_2}{b}, \gamma = \frac{K_{R2}}{K_{R1}}, \alpha_D = \frac{\alpha_{R2}}{\alpha_{R1}}, q_D = \frac{\rho_A c_A Q}{2\pi b K_{r1}}, t_D = \frac{\alpha_{R1} t}{b^2} \tag{18}$$

The Laplace-domain solutions of Eqs. (13), (16), and (17) in dimensionless form are respectively

$$\overline{T}_{AD}(r_D, s) = \left(\frac{1}{s} - \frac{A_{2D}(s)}{sA_{1D}(s)}\right) \exp\left\{\left(\frac{-1}{2q_D}\right) A_{1D}(s)\left(r_D^2 - r_{wD}^2\right)\right\} + \frac{A_{2D}(s)}{sA_{1D}(s)} \tag{19}$$

$$\overline{T}_{R1D}(r_D, z_D, s) = \frac{\sinh(q_{1D}(b_{1D} + z_D))}{\sinh(q_{1D} b_{1D})}\left(\overline{T}_{AD}(r_D, s) - \frac{T_{R10D}}{s}\right) + \frac{T_{R10D}}{s} \tag{20}$$

and

$$\overline{T}_{R2D}(r_D, z_D, s) = \frac{\sinh(q_{2D}(1 + b_{2D} - z_D))}{\sinh(q_{2D} b_{2D})}\left(\overline{T}_{AD}(r_D, s) - \frac{T_{R20D}}{s}\right) + \frac{T_{R20D}}{s} \tag{21}$$

with

$$A_{1D}(s) = q_{1D}\coth(q_{1D} b_{1D}) + \gamma q_{2D}\coth(q_{2D} b_{2D}) \tag{22}$$

and

$$A_{2D}(s) = q_{1D}\coth(q_{1D} b_{1D}) T_{R10D} + \gamma q_{2D}\coth(q_{2D} b_{2D}) T_{R20D} \tag{23}$$

where $q_{1D}^2 = s$ and $q_{2D}^2 = s/\alpha_D$.

When T_{A0}=T_{R10}=T_{R20}, there is no geothermal gradient in the reservoir. Thus, one can obtain T_{R10D}=T_{R20D}=0 and A_2 (s)=0. The Laplace-domain solutions of Eqs. (13), (16), and (17) are then reduced to

$$\overline{T}_{AD}(r, s) = \frac{1}{s}\exp\left\{\left(\frac{-\pi}{\rho_A c_A Q}\right) A_1(s)\left(r^2 - r_w^2\right)\right\} \tag{24}$$

$$\overline{T}_{R1D}(r, z, s) = \frac{\sinh(q_1(b_1 + z))}{\sinh(q_1 b_1)}\overline{T}_{AD}(r, s) \tag{25}$$

and

$$\overline{T}_{R2D}(r, z, s) = \frac{sinh(q_2(b + b_2 - z))}{\sinh(q_2 b_2)}\overline{T}_{AD}(r, s) \tag{26}$$

If the underlying and overlying rocks have the same finite thickness, b_R, and physical and thermal properties, then T_{R1}=T_{R2}=T_R, $\alpha_{R1} = \alpha_{R2} = \frac{K_R}{\rho_R c_R}$, q_1=q_2=q, and $A_1(s) = 2K_R q\coth(qb_R)$. Accordingly, Eq. (24) becomes

$$\overline{T}_{AD}(r, s) = \frac{1}{s}\exp\left\{\left(\frac{-\pi}{\rho_A c_A Q}\right)(2K_R q\coth(qb_R))\left(r^2 - r_w^2\right)\right\} \tag{27}$$

which is similar to the solution of Bodvarsson and Tsang (1982) derived based on the assumption that there is no heat flow at the upper and lower boundaries.

If the thicknesses of the underlying and overlying rocks is very large and considered as infinite, then $\coth(qb_R)$ is equal to one. Under this circumstance, Eq. (27) can be simplified as

$$\overline{T}_{AD}(r, s) = \frac{1}{s}\exp\left\{\left(\frac{-\pi}{\rho_A c_A Q}\right)(2K_R q)\left(r^2 - r_w^2\right)\right\} \tag{28}$$

Numerical evaluations

Equation (13) is a function of the hyperbolic cotangent and is rather complicated. Thus, its analytical solution in time domain may not be tractable. Similarly, the analytical solutions of Eqs. (16) and (17) may not be available either. Equations (13), (16), and (17) are therefore numerically inverted by the routine INLAP of IMSL (1997) with an accuracy to four significant figures. This routine was developed based on a numerical algorithm originally proposed by Crump (1976) and modified by de Hoog et al. (1982). This algorithm approximates the Laplace inversion by expressing the inverted function in a Fourier series and accelerates the evaluation by the Shanks method (Shanks 1955; Peng et al. 2002).

Equations (16) and (17) include the functions of hyperbolic sine, $\sinh(z)$, and hyperbolic cotangent, $\coth(z)$. The $\sinh(z)$ becomes infinite as z approaches infinity. The numerical evaluation for $\sinh(z_1)/\sinh(z_2)$ may diverge when z_1 and/or z_2 become very large. Using the series representations for $\sinh(z_1)$ and $\sinh(z_2)$ (Abramowitz and Stegun 1964, p. 85), the term $\sinh(z_1)/\sinh(z_2)$ after taking long division becomes

$$\frac{\sinh(z_1)}{\sinh(z_2)} = \sum_{i=1}^{\infty}\left[e^{z_1 - (2i-1)z_2} - e^{-z_1 - (2i-1)z_2}\right] \tag{29}$$

Equation (29) converges if $z_1 \leq z_2$. The infinite sum on the right-hand side of Eq. (29) can be evaluated by the Shanks method to accelerate convergence. This method has been successfully applied to efficiently solve many

 DOI 10.1007/s10040-008-0327-9

problems in the groundwater area (see, e.g., Yang and Yeh 2002; Yeh et al. 2003).

Results and discussions

The effects of the well radius, reservoir thickness, and pumping flow rate on the aquifer temperature are examined hereinafter. The data used in the following simulations are $\rho_A c_A = 2.5 \times 10^6 J/m^3 \cdot^\circ C$, b=20 m, $\rho_{R1} c_{R1} = 2.7 \times 10^6 J/m^3 \cdot^\circ C$, K_{R1}=2.5 W/m°C, b_1=20 m, $\rho_{R2} c_{R2} = 2.3 \times 10^6 J/m^3 \cdot^\circ C$, K_{R2}=1.5 W/m°C, and b_2=50 m. The injection well is fully penetrating with a radius r_w of 0.05 m. Assume that the initial temperatures are T_{A0}=33°C for the aquifer, T_{R10}=34°C for the underlying rock, and T_{R20}=32°C for the overlying rock. The temperature of the injected water is maintained at T_{w0}=50°C and the injection rate is Q=10^{-4} m^3/s or 5×10^{-4} m^3/s.

Figure 2 shows the effects of the radial distance, injected time, and injected flow rate on the aquifer temperature. In Fig. 2 the solid and dotted lines denote the aquifer temperature for the cases of injection rate $Q = 1 \times 10^{-4} m^3/s$ and 5×10^{-4} m^3/s, respectively. This figure shows that the aquifer temperature decreases significantly with increasing radial distance for a fixed time and flow rate. On the other hand, the aquifer temperature increases significantly with the flow rate if the radial distance and time are kept constant. For fixed flow rates, the aquifer temperature increases significantly with time at a small radial distance and slowly at a large radial distance. The aquifer temperature approaches the initial aquifer temperature (T_{A0}) at a very large distance and/or after a long period of injection. The effect of the injected hot water on the aquifer temperature at a large distance is negligible and the radius of influence of the ATES system is about 30 m when $Q = 1 \times 10^{-4} m^3/s$ and 60 m when $Q = 5 \times 10^{-4} m^3/s$.

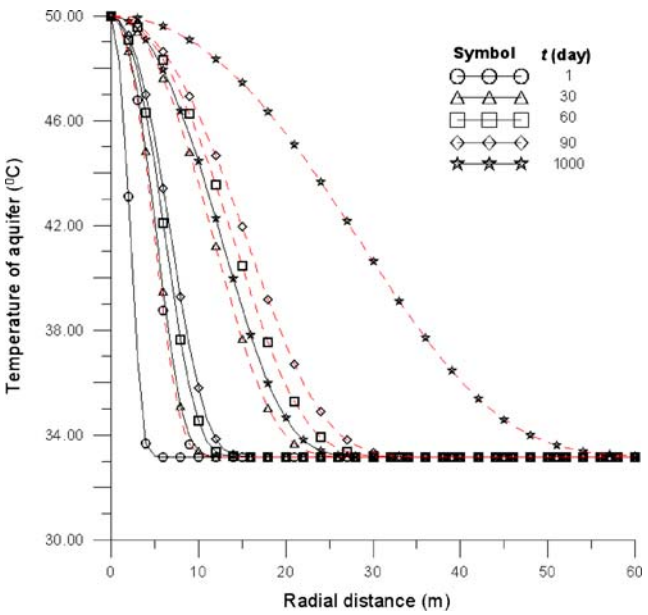

Fig. 2 Plots of aquifer temperature T_A versus radial distance r for $Q = 1 \times 10^{-4}$ and $5 \times 10^{-4} m^3/s$ when t=1, 30, 60, 90 or 1,000 days. The *solid and dotted lines* denote the aquifer temperature for the cases of the injection flow rate $Q = 1 \times 10^{-4} m^3/s$ and 5×10^{-4} m^3/s, respectively

Figure 3 shows the temperature distribution contour for the ATES system with $Q = 5 \times 10^{-4} m^3/s$ at t=30, 60 or 90 days. Note those irregularities in the contour lines shown in Fig. 3 are mainly caused by the surface mapping software Surfer (Golden Software 1999), not by the behavior of the temperature distributions. The radius of influence is defined as a distance from the injection well to the location where the temperature increase is equal to 0.5°C. Figure 3a indicates the radius of influence for the aquifer is about 26 m when t=30 days. In addition, the temperature radiuses of influence within the rocks are z_1=−8 m for the underlying rock and z_2=26 m for the overlying rock. The radius of influence for the aquifer is about 29 m when t=60 days as shown in Fig. 3b. The temperature radiuses of influence within the rocks are z_1=−10 m for the underlying rock and z_2=28 m for the overlying rock. Figure 3c indicates the radius of influence for the aquifer is about 20 m when t=90 days. This distance is significantly smaller than that when t=60 days due to the water flow velocity is very small at this distance and the heat transfer replaces the heat migration exerting the temperature distribution at the interface. The temperature radiuses of influence are z_1=−8 m for the underlying rock and z_2=28 m for the overlying rock. The temperature radiuses of influence compared with those when t=60 days for the rocks are not changed in the radius of influence. In addition, the effects of the rocks on the temperature distribution increase with time at large radial distance. Those results show that the effect of the hot water injection on the temperature distribution is significant for the aquifer and is very minor for the rocks at a short period of time. It indicates that the migration of hot water in the aquifer is quick and the heat transfer in the rock is slow. In addition, the heat transfer in the aquifer and rocks increases with time and decreases with increasing r and z.

Figure 4 shows the radius of influence versus temperature for an ATES system with $Q = 5 \times 10^{-4} m^3/s$ for t ranging from 1 to 1,000 days. The results show that the radius of influence increases dramatically at small time and slowly at large time. The radius of influence in the aquifer is larger than those in the overlying and underlying rocks at all test times. In addition, the radius of influence in the underlying rock is larger than that in the overlying rock. It illustrates that a larger thermal diffusivity of the rock results in a longer radius of influence. These results also show that the influence of the injection of hot water on the formation temperature distribution is more significant in the aquifer than that in the overlying/underlying rocks. It indicates that the heat transfer is faster in the aquifer than in the overlying/underlying rocks. In addition, the heat transfers in the aquifer and rocks increases with

 DOI 10.1007/s10040-008-0327-9

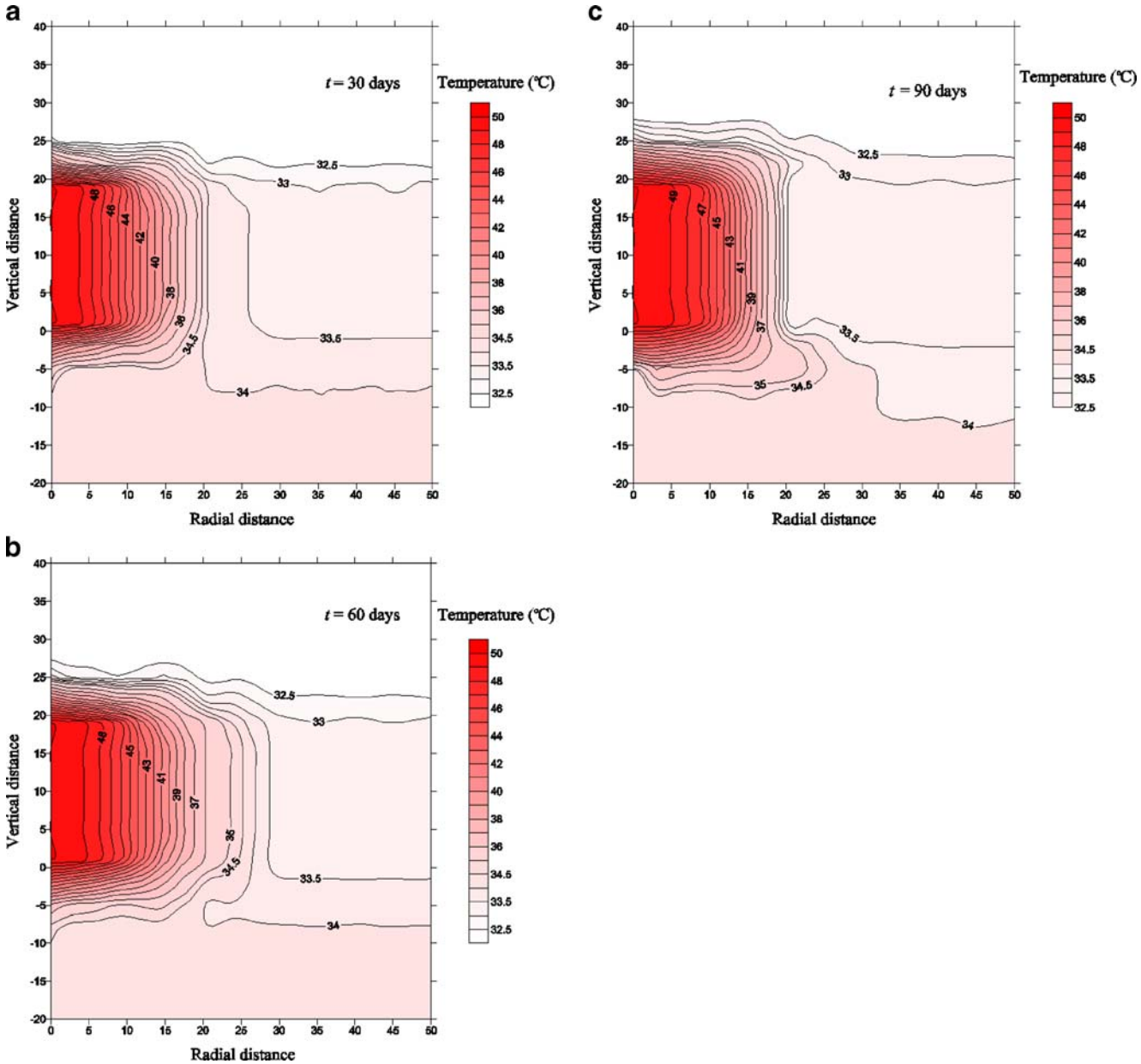

Fig. 3 Contour plots of the temperature distribution in an ATES system for $Q = 5 \times 10^{-4} m^3/s$ when **a** t=30 days, **b** t=60 days, and **c** t=90 days

time and decreases with increasing horizontal and vertical distances.

The field data of the geothermal system at Susanville, California (Bodvarsson et al. 1982) is adopted to demonstrate the application of the present model. The parameters used in their simulation were $\rho_A c_A = 2.989 \times 10^6 J/m^3 \cdot ^\circ C$, b=35 m, $\rho_{R1} c_{R1} = \rho_{R2} c_{R2} = 2.7 \times 10^6 J/m^3 \cdot ^\circ C$, and K_{R1}=K_{R2}=1.5 W/m°C. In simulating an ATES system, the temperature of injection water is fixed at T_{w0}=80°C and the thicknesses of the underlying and overlying rocks are b_1=50 m and b_2=40 m, respectively. Assume that the initial temperatures are T_{A0}=40°C for the aquifer and T_{R10}=41°C and T_{R20}=39°C for the underlying and overlying rocks, respectively. Note that the geothermal gradients in both the underlying and overlying rocks are neglected since the thicknesses of the rocks are not large. The flow rate of recharge is Q=0.035 m^3/s in this ATES system. Figure 5 shows the radius-temperature curve when the recharging time t=0.1, 1, 10, 100 years. It shows that the aquifer temperature decreases significantly with increasing radial distance and approaches the initial aquifer temperature at a very large distance. If the limiting temperature is taken as 60°C, the radiuses of influence are 200, 300, 400, and 600 m after 0.1, 1, 10 or 100 years, respectively. This result can be used to predict the area extent and amount of hydrothermal energy for the ATES system.

Those results demonstrate that the present model can be used to assess the effects of the injection of hot water

 DOI 10.1007/s10040-008-0327-9

on the temperature distribution in an ATES system. This model has practical use for designing the ATES system.

Conclusions

A mathematical model describing the thermal energy transport in a confined aquifer in an ATES system is presented. The Laplace-domain solutions for the temperature distribution are derived by the Laplace transforms and the corresponding solutions in time domain are evaluated using the modified Crump method. The conclusions of this study can be stated as follows:

1. The present model can be used to estimate the effects of hot water injection on the temperature distribution in an ATES system for various radial distances, injection times, and injection flow rates. It is useful in the design of efficient ATES facilities when injecting hot water into a confined aquifer for the storage or the disposal of waste heat energy.
2. The effect of hot water injection on the temperature distribution in the aquifer is significant during a short period of injection time. In contrast, the temperature distributions in overlying and underlying the rocks are affected only after a long period of injection time.
3. The temperatures in the aquifer and the underlying and overlying rocks increase with time and decrease with increasing radial and vertical distances. The effect of hot water injection on the temperature distribution increases with injection flow rate and water temperature.
4. The radius of influence in an ATES system depends on the physical and thermal properties, injection flow rate, and injection water temperature. The radius of influence increases dramatically for small injection times and slowly for long periods of injection time. In addition, a larger value of the thermal diffusivity or injection flow rate gives a longer radius of influence.

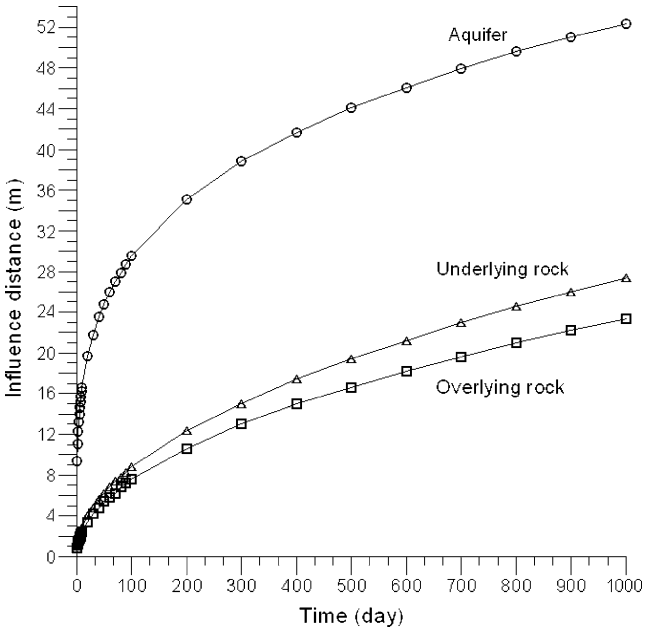

Fig. 4 Radius of influence in the aquifer, underlying rock, and overlying rock for $Q = 5 \times 10^{-4} m^3/s$ when t ranges from 1 to 1,000 days

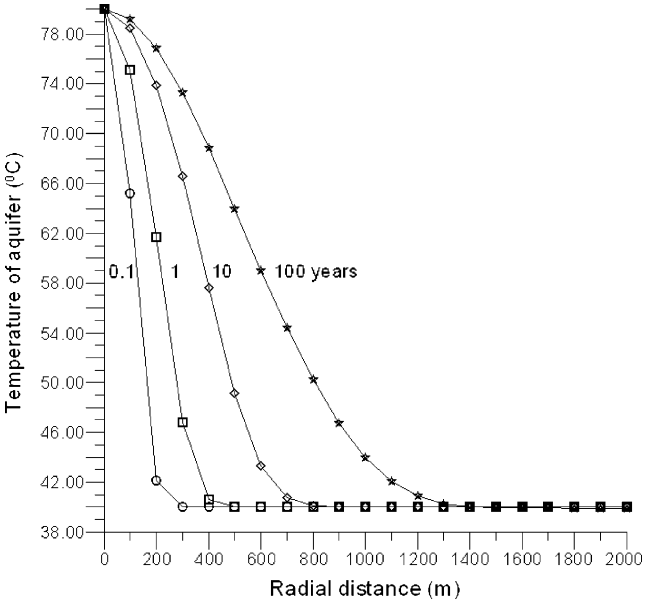

Fig. 5 Plots of aquifer temperature T_A versus radial distance r for $\rho_A c_A = 2.989 \times 10^6 J/m^3 \cdot^\circ C$, b=35 m, $\rho_{R1}c_{R1} = \rho_{R2}c_{R2} = 2.7 \times 10^6 J/m^3 \cdot^\circ C$, K_{R1}=K_{R2}=1.5 W/m°C, b_1=b_2=125 m, T_{w0}=80°C, T_{A0}=40°C, T_{R10}=41°C, T_{R20}=39°C, and Q=0.035 m^3/s in a hydrothermal system when t=0.1, 1, 10 or 100 years

Acknowledgements Research leading to this paper has been partially supported by the grants from Taiwan National Science Council under the contract number NSC 96-2221-E-238-009.

Appendix

The coupled boundary value problem represented by Eqs. (1)–(11) can be expressed in a dimensionless form based on the dimensionless groupings of Eq. (12). For the aquifer, the governing equation for the steady-state heat conduction is

$$(b\rho_A c_A)\left(\frac{Q}{2\pi r b}\right)\frac{\partial T_{AD}(r,t)}{\partial r} = -K_{R1}\left.\frac{\partial T_{R1D}(r,z,t)}{\partial z}\right|_{z=0} + K_{R2}\left.\frac{\partial T_{R2D}(r,z,t)}{\partial z}\right|_{z=b} \quad (30)$$

The initial condition is

$$T_{AD}(r,0) = 0 \quad (31)$$

The boundary condition at the rim of wellbore is

$$T_{AD}(r_w,t) = 1 \quad (32)$$

 DOI 10.1007/s10040-008-0327-9

For the underlying rock, the heat conduction equation is

$$\frac{\partial^2 T'_{R1D}(r,z,t)}{\partial z^2} = \frac{1}{\alpha_{R1}} \frac{\partial T'_{R1D}(r,z,t)}{\partial t}, \alpha_{R1} = \frac{K_{R1}}{\rho_{R1} c_{R1}} \quad (33)$$

The initial condition is

$$T'_{R1D}(r,z,0) = 0 \quad (34)$$

The boundary conditions are

$$T'_{R1D}(r,0,t) = T_{AD}(r,t) - T_{R10D} \quad (35)$$

and

$$T'_{R1D}(r,-b_1,t) = 0 \quad (36)$$

For the overlying rock, the heat conduction equation for the temperature distribution can be written as

$$\frac{\partial^2 T'_{R2D}(r,z,t)}{\partial z^2} = \frac{1}{\alpha_{R2}} \frac{\partial T'_{R2D}(r,z,t)}{\partial t}, \alpha_{R2} = \frac{K_{R2}}{\rho_{R2} c_{R2}} \quad (37)$$

The initial condition is

$$T'_{R2D}(r,z,0) = 0 \quad (38)$$

The boundary conditions are

$$T'_{R2D}(r,b,t) = T_{AD}(r,t) - T_{R20D} \quad (39)$$

and

$$T'_{R2D}(r,b+b_2,t) = 0 \quad (40)$$

Applying Laplace transforms to Eqs. (30)–(40), the governing equation for the aquifer becomes

$$\left(\frac{\rho_A c_A Q}{2\pi}\right)\left(\frac{1}{r}\frac{d\overline{T}_{AD}(r,s)}{dr}\right) = -K_{R1}\frac{d\overline{T}_{R1D}(r,z,s)}{dz}\bigg|_{z=0} + K_{R2}\frac{d\overline{T}_{R2D}(r,z,s)}{dz}\bigg|_{z=b} \quad (41)$$

and the boundary condition becomes

$$\overline{T}_{AD}(r_w,s) = \frac{1}{s} \quad (42)$$

The heat conduction equation for the underlying rock results in

$$\frac{d^2 \overline{T}'_{R1D}(r,z,s)}{dz^2} = q_1^2 \overline{T}'_{R1D}(r,z,s), q_1^2 = \frac{s}{\alpha_{R1}} \quad (43)$$

and the related boundary conditions are

$$\overline{T}'_{R1D}(r,0,s) = \overline{T}_{AD}(r,s) - \frac{T_{R10D}}{s} \quad (44)$$

and

$$\overline{T}'_{R1D}(r,-b_1,s) = 0 \quad (45)$$

The heat conduction equation for the overlying rock becomes

$$\frac{d^2 \overline{T}'_{R2D}(r,z,s)}{dz^2} = q_1^2 \overline{T}'_{R2D}(r,z,s), q_2^2 = \frac{s}{\alpha_{R2}} \quad (46)$$

and the related boundary conditions are

$$\overline{T}'_{R2D}(r,b,s) = \overline{T}_{AD}(r,s) - \frac{T_{R20D}}{s} \quad (47)$$

and

$$\overline{T}'_{R2D}(r,b+b_2,s) = 0 \quad (48)$$

Substituting Eqs. (44) and (45) into Eq. (43) yields

$$\overline{T}'_{R1D}(r,z,s) = \frac{\sinh(q_1(b_1+z))}{\sinh(q_1 b_1)}\left(\overline{T}_{AD}(r,s) - \frac{T_{R10D}}{s}\right) \quad (49)$$

Based on Eq. (12), Eq. (49) can be rewritten as

$$\overline{T}_{R1D}(r,z,s) = \frac{\sinh(q_1(b_1+z))}{\sinh(q_1 b_1)}\left(\overline{T}_{AD}(r,s) - \frac{T_{R10D}}{s}\right) + \frac{T_{R10D}}{s} \quad (50)$$

Similarly, the Laplace-domain solution for the underlying rock can be obtained by substituting Eqs. (47) and (48) into Eq. (46) as

$$\overline{T}'_{R2D}(r,z,s) = \frac{\sinh(q_2(b+b_2-z))}{\sinh(q_2 b_2)}\left(\overline{T}_{AD}(r,s) - \frac{T_{R0D}}{s}\right) \quad (51)$$

The above equation can be rewritten by the use of Eq. (12) as

$$\overline{T}_{R2D}(r,z,s) = \frac{\sinh(q_2(b+b_2-z))}{\sinh(q_2 b_2)}\left(\overline{T}_{AD}(r,s) - \frac{T_{R0D}}{s}\right) + \frac{T_{R0D}}{s} \quad (52)$$

The substitution of Eqs. (50) and (52) into Eq. (41) yields

$$\left(\frac{\rho_A c_A Q}{2\pi}\right)\left(\frac{1}{r}\frac{d\overline{T}_{AD}(r,s)}{dr}\right) = -K_{R1} q_1 \coth(q_1 b_1)\left(\overline{T}_{AD}(r,s) - \frac{T_{R10D}}{s}\right) - K_{R2} q_2 \coth(q_2 b_2)\left(\overline{T}_{AD}(r,s) - \frac{T_{R20D}}{s}\right) \quad (53)$$

After substituting Eq. (42) into Eq. (53), the Laplace-domain solution, Eq. (13), can then be obtained.

 DOI 10.1007/s10040-008-0327-9

References

Abramowitz M, Stegun IA (1964) Handbook of mathematical functions with formulas, graphs and mathematical tables. National Bureau of Standards, Washington, DC

Bodvarsson GS, Tsang CF (1982) Injection and thermal breakthrough in fractured geothermal reservoirs. J Geophys Res 87 (B2):1031–1048

Bodvarsson GS, Benson SM, Witherspoon PA (1982) Theory of the development of geothermal systems charged by vertical faults. J Geophys Res 87(B11):9317–9328

Carslaw HS, Jaeger JC (1959) Conduction of heat in solids, 2nd edn. Clarendon, Oxford, UK

Chen CS, Reddell DL (1983) Temperature distribution around a well during thermal injection and a graphical technique for evaluating aquifer thermal properties. Water Resour Res 19 (2):351–363

Cheng P, Teckchandani L (1977) Numerical solutions for transient heating and fluid withdrawal in a liquid-dominated geothermal reservoir. In: The Earth's crust: its nature and physical properties, AGU monograph vol 20, AGU, Washington, DC, pp 705–721

Cheng AH-D, Ghassemi A, Detournay E (2001) Integral equation solution of heat extraction from a fracture in hot rock. Int J Numer Anal Methods Geomech 25:1327–1338

Chevalier S, Banton O (1999a) Modelling of heat transfer with the random walk method. Part 1. Application to thermal energy storage in porous aquifers. J Hydrol 222:129–139

Chevalier S, Banton O (1999b) Modelling of heat transfer with the random walk method. Part 2. Application to thermal energy storage in fractured aquifers. J Hydrol 222:140–151

Crump KS (1976) Numerical inversion of Laplace transforms using a Fourier series approximation. J Assoc Comput Mach 23 (1):89–96

de Hoog FR, Knight JH, Stokes AN (1982) An improved method for numerical inversion of Laplace transforms, society for industrial and applied mathematics. J Sci Stat Comput 3(3):357–366

Golden Software (1999) Surfer, version 7.00, Golden Software, Golden, CO, USA

IMSL (1997) Stat/Library, vols 1 and 2, Visual numerics, IMSL, Houston, TX, USA

Molson JW, Frind EO, Palmer CD (1992) Thermal energy storage in an unconfined aquifer: 2. model development, validation, and application. Water Resour Res 28(10):2857–2867

Nagano K, Mochida T, Ochifuji K (2002) Influence of natural convection on forced horizontal flow in saturated porous media for aquifer thermal energy storage. Appl Therm Eng 22:1299–1311

Noyer ML (1977) Simulations des transferts thermiques dans les aquiferes. Conditions de validite des solutions analytiques. Rap-BRGM 77 SGN 598 HYD, BRGM, Orléans, France, 33 pp

Paksoy HO, Gurbuz Z, Turgut B, Dikici D, Evliya H (2004) Aquifer thermal storage (ATES) for air-conditioning of a supermarket in Turkey. Renew Energy 29:1991–1996

Palmer CD, Blowes DW, Frind EO, Molson JW (1992) Thermal energy storage in an unconfined aquifer: 1. field injection experiment. Water Resour Res 28(10):2845–2856

Peng HY, Yeh HD, Yang SY (2002) Improved numerical evaluation for the radial groundwater flow equation. Adv Water Resour 25 (6):663–675

Özisik MN (1993) Heat conduction, 2nd edn. Wiley, New York

Shanks D (1955) Non-linear transformations of divergent and slowly convergent sequences. J Math Phys 34:1–42

Spiegel MR (1965) Laplace transforms. Schaum, New York

Stehfest H (1970) Numerical inversion of Laplace transforms. Commun ACM 13(1):47–49

Stopa J, Wojnarowski P (2006) Analytical model of cold water front movement in a geothermal reservoir. Geothermics 35:59–69

Yang SY, Yeh HD (2002) Solution for flow rates across the wellbore in a two-zone confined aquifer. J Hydraul Eng ASCE 128 (2):175–183

Yeh HD, Yang SY, Peng HY (2003) A new closed-form solution for radial two-layer drawdown equation under constant-flux pumping in a finite-radius well. Adv Water Resour 26(5):747–757

Ziagos JP, Blackwell DD (1986) A model for the transient temperature effects of horizontal fluid flow in geothermal systems. J Volcanol Geotherm Res 27:371–397

 DOI 10.1007/s10040-008-0327-9